# Application of an Adiabatic WRF Adjoint to the Investigation of the May 2004 McMurdo, Antarctica, Severe Wind Event

QINGNONG XIAO, YING-HWA KUO, ZAIZHONG MA, WEI HUANG, XIANG-YU HUANG, XIAOYAN ZHANG, DALE M. BARKER, JOHN MICHALAKES, AND JIMY DUDHIA

*National Center for Atmospheric Research,* Mesoscale and Microscale Meteorology Division, Boulder, Colorado*

(Manuscript received 19 April 2007, in final form 25 February 2008)

ABSTRACT

The tangent linear and adjoint of an adiabatic version of the Weather Research and Forecasting (WRF) Model with its Advanced Research WRF (ARW) dynamic core have been developed. The source-to-source automatic differentiation tool [i.e., the Transformation of Algorithm (TAF) in FORTRAN] was used in the development. Tangent linear and adjoint checks of the developed adiabatic WRF adjoint modeling system (WAMS) were conducted, and all necessary correctness verification procedures were passed. As the first application, the adiabatic WAMS was used to study the adjoint sensitivity of a severe windstorm in Antarctica. Linearity tests indicated that an adjoint-based sensitivity study with the Antarctic Mesoscale Prediction System (AMPS) 90-km domain configuration for the windstorm is valid up to 24 h. The adjoint-based sensitivity calculation with adiabatic WAMS identified sensitive regions for the improvement of the 24-h forecast of the windstorm. It is indicated that the windstorm forecast largely relies on the model initial conditions in the area from the south part of the Trans-Antarctic Mountains to West Antarctica and between the Ross Ice Shelf and the South Pole. Based on the sensitivity analysis, the southerly or southeasterly wind at lower levels in the sensitivity region should be larger, the cyclone should be stronger, and the atmospheric stratification should be more stable over the north slope of the Trans-Antarctic Mountain to the Ross Ice Shelf, than the AMPS analyses. By constructing pseudo-observations in the sensitivity region using the gradient information of forecast windstorm intensity around McMurdo, the model initial conditions are revised with the WRF three-dimensional variational data assimilation, which leads to significant improvement in the prediction of the windstorm. An adjoint sensitivity study is an efficient way to identify sensitivity regions in order to collect more observations in the region for better forecasts in a specific aspect of interest.

## 1. Introduction

A common problem in Antarctic weather prediction is sparse observational data in the area. The lack of observations significantly increases uncertainties in the model initial conditions and results in inferior forecast skill, as compared with that in the highly populated midlatitudes of the Northern Hemisphere (Bromwich and Cassano 2001). In the summer, approximately one dozen radiosonde stations operate over the entire Antarctic continent. In the winter, the number is further reduced. With the exception of the South Pole station, all the radiosonde stations are located on the periphery of the continent. Moreover, except for a few island stations, there are virtually no upper-air stations over the Southern Ocean. Although there are approximately 100 automatic weather stations (AWSs) over the continent, most AWS data are not included in the routine global telecommunication system (GTS) transmissions, and are therefore not available for real-time operational analysis. Currently, several types of satellite observations are available over Antarctica and its surrounding area. However, their usage is limited because of the data contamination by persistent clouds, precipitation, and surface ice over Antarctica and the Southern Ocean. The accuracy of the retrieval algorithms and the effectiveness of various assimilation approaches/strategies for the Antarctic area need further testing and improvement.

* The National Center for Atmospheric Research is sponsored by the National Science Foundation.

*Corresponding author address:* Dr. Qingnong Xiao, National Center for Atmospheric Research, Mesoscale and Microscale Meteorology Division, P. O. Box 3000, Boulder, CO 80307-3000.
E-mail: hsiao@ucar.edu

DOI: 10.1175/2008MWR2235.1

© 2008 American Meteorological Society

Despite difficulties in meteorological analysis in Antarctica, great effort has been made to improve the weather forecasting in the region. Antarctic weather prediction is performed by various nations to facilitate scientific activities on the continent. In support of the flight operations of the U.S. Antarctic Program, the National Center for Atmospheric Research partnered with the Byrd Polar Research Center at Ohio State University to develop the Antarctic Mesoscale Prediction System (AMPS; Powers et al. 2003). AMPS has provided experimental real-time numerical forecasts for Antarctica since September 2000. Although originally developed with the fifth-generation Pennsylvania State University–National Center for Atmospheric Research (NCAR) Mesoscale Model (MM5; Dudhia 1993; Grell et al. 1995), the Weather Research and Forecasting (WRF) Model (Skamarock et al. 2005) has recently been adapted to AMPS as the next-generation mesoscale modeling system for Antarctica.

Numerical weather prediction is important for base operations at McMurdo Station in the Ross Island of Antarctica, because it is the logistical hub and the largest base of the U.S. Antarctic Program. On 15 May 2004, a severe windstorm hit the McMurdo Station area. It damaged a lot of facilities and impeded research activities at the station. The most intense wind gust recorded from this event was over 71 m $s^{-1}$. It was one of the most severe wind events to strike McMurdo Station in recorded history (Powers 2007; Steinhoff et al. 2008).

Accurate forecasting of such a storm is very difficult with limited observations to properly describe the atmospheric state in Antarctica. It is also unrealistic to deploy a dense surface-based observation network in Antarctica to improve its analysis of the atmospheric state in the foreseeable future. In such an environment, it would be desirable to identify the forecast sensitivity region and sensitivity parameters in the region that could contribute to a significant improvement for weather forecasting at McMurdo. Through such sensitivity studies one can concentrate resources to take observations that are the most useful in improving the weather prediction over a specific target area (e.g., the McMurdo Station).

During the past several years, NCAR has been active in the development of the WRF adjoint modeling system (WAMS). An adjoint sensitivity study of initial conditions to the model forecasts is a very useful approach to identify the locations and variables in the analyses that have significant influence on the model forecast over a specific area (Errico and Vukicevic 1992; Rabier et al. 1996; Langland et al. 1999; Li et al. 1999; Xiao et al. 2002; Kleist and Morgan 2005a,b). It is a computationally efficient method to determine the sensitivity of the model forecast's response to the model initial conditions. It can be used to locate high-sensitivity regions and atmospheric parameters in which small perturbations can have a relatively large effect on specific forecast features. Such a sensitivity analysis will provide guidance on the strategies for observation data collection and observing system deployment. In a previous study, Xiao et al. (2002) performed an adjoint sensitivity study for a cyclone during the North Pacific Experiment (NORPEX) using the MM5 adjoint modeling system (Zou et al. 1997). It was found that the prediction of the mid-Pacific Ocean cyclone was sensitive to the wind field over the East Asia coast and northwest Pacific region. The cyclone intensity was more sensitive to winds at lower levels than at higher levels. Data impact studies from NORPEX showed a ~10% reduction in mean 2-day forecast errors over western North America from the assimilation of targeted dropsondes and satellite wind data (Langland et al. 1999). The development of WAMS provides an opportunity to test adjoint sensitivity in the May 2004 McMurdo severe wind event (described in Steinhoff et al. 2008). Such an application can reveal some new insight into the cause of the event, and provide guidance for the collection and deployment of observations to improve the prediction skill of such an event in the future.

This paper is arranged as follows: the next section will provide descriptions and synopsis of the May 2004 McMurdo severe wind event. Section 3 briefly documents the adiabatic WAMS development and its correctness verification. The WRF control experiments with the AMPS analysis using NCEP Global Forecast System (GFS) data and its 24-h linearity test are presented in section 4. We describe the adjoint sensitivity analysis for the event in section 5. Numerical results using the adjoint gradient information to improve the forecast of the event are presented in section 6. A summary and conclusions are provided in section 7.

## 2. Synoptic overview of the May 2004 McMurdo severe wind event

The event occurred on 15 May 2004 in the McMurdo Station area in Antarctica (see Fig. 1 for the location). Synoptic analysis indicated that the windstorm was caused by the passage of an Antarctic cyclone. At 0000 UTC 14 May the cyclone was originated over the Amundsen Sea (see Fig. 1 for the location) and moved to the western Marie Byrd Land late on 14 May (Fig. 2).

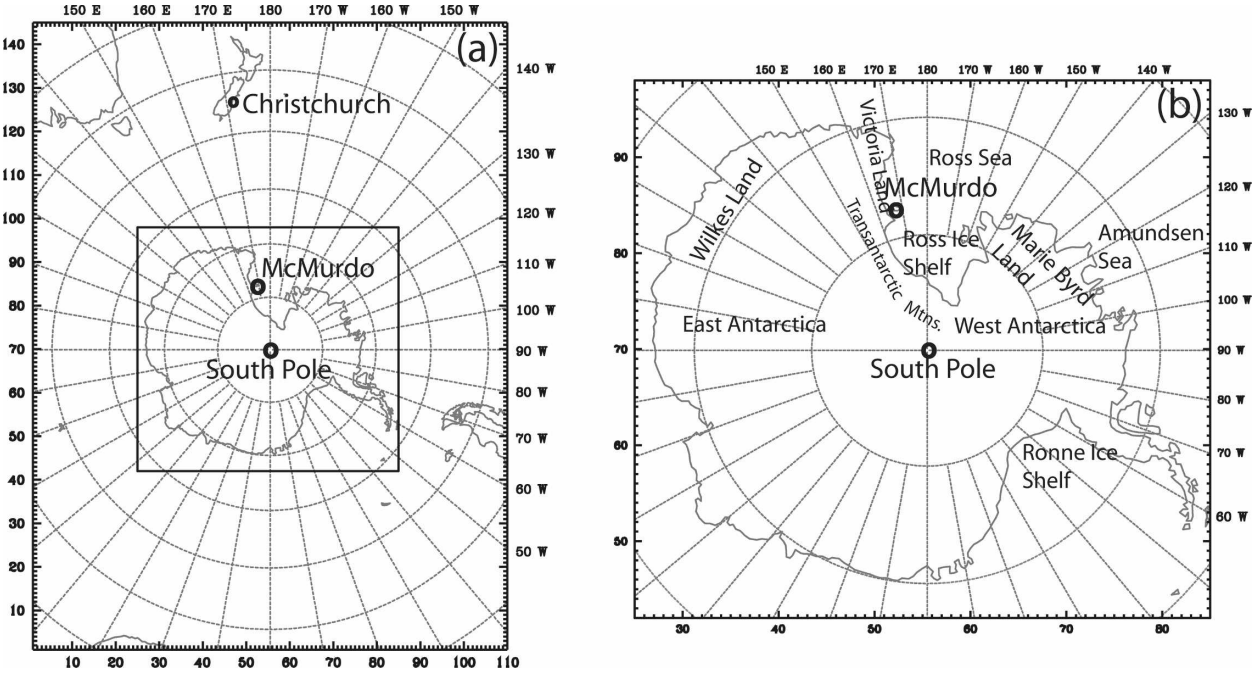


FIG. 1. Model domain configurations and key Antarctic locations. (a) The domain with 90-km grid for all experiments in this paper. (b) The subdomain in (a) for description of the adjoint sensitivity experiments. The key geographical locations (i.e., the McMurdo Station and the South Pole) are shown with black circles.

From 0700 to 1000 UTC 15 May it crossed the Spine Coast and moved westward across the Ross Ice Shelf. At 1500 UTC it approached the date line and began a northward turn. McMurdo experienced the strongest winds from 1800 UTC 15 May to 0000 UTC 16 May, and the low's positions during this period were to the southeast and east of Ross Island and McMurdo as shown in Fig. 2. During the passage of the cyclone, the strong pressure gradient to the west of the low yielded an intense southerly flow. The strong southerly inflow over the Trans-Antarctic Mountains, together with a favorable environment, induced severe downslope winds over the Ross Sea. The McMurdo area was badly hit by the severe windstorm from 1800 UTC 15 May. After 0000 UTC 16 May, the cyclone gradually weakened and moved northward to the Terra Nova Bay region.

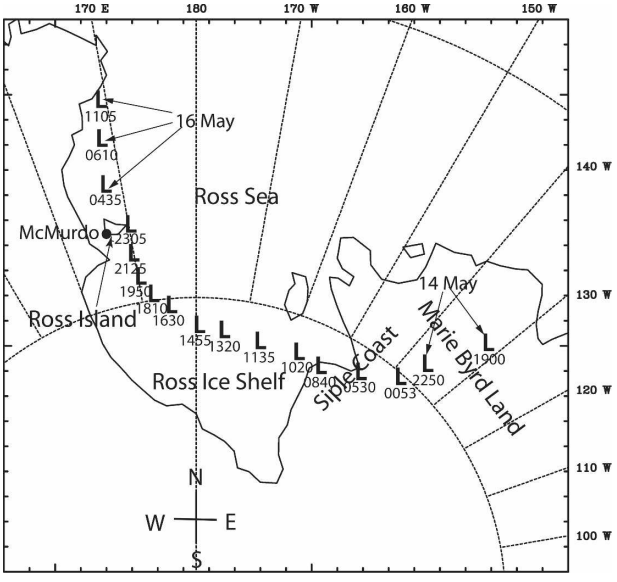


FIG. 2. Track of the observed low determined through analysis of satellite imagery. Times (UTC) of central position of the low (marked "L") are indicated. Courtesy of Powers (2007).

## 3. Brief description of the adiabatic WRF adjoint modeling system

During the past several years, significant efforts at NCAR have been devoted to the WAMS development. With the help of the automatic differentiation software [i.e., the Transformation of Algorithm (TAF) in FORTRAN; Giering and Kaminski 2003], the WRF tangent linear and adjoint models have been successfully coded, based on an adiabatic version of the Advanced Research WRF dynamic core (WRF-ARW; Skamarock et al. 2005). There are three phases in developing the system. First, numerical experiments were

conducted to make sure the adiabatic version of WRF with simple diffusion and surface drag can reproduce the major features that the full-physics model does. Second, the tangent linear model and its adjoint were generated using TAF. The final step was to verify the correctness of the tangent linear and adjoint models.

### a. Adiabatic version of WRF with vertical diffusion and surface drag

WRF is a sophisticated and fairly complicated model. It has a fully compressible, Euler nonhydrostatic solver with conservation of scalar variables. The prognostic variables are velocity components $u$ and $v$ in Cartesian coordinates, vertical velocity $w$, perturbation potential temperature, perturbation geopotential, perturbation surface pressure of dry air, and scalars of water vapor mixing ratio and other hydrometeor mixing ratios (i.e., rain/snow, cloud water/ice, etc.).

The model equations are formulated using a terrain-following hydrostatic pressure vertical coordinate denoted by $\eta$ and defined as

$$\eta = \frac{p_h - p_{ht}}{\mu}, \tag{1}$$

where $\mu = p_{hs} - p_{ht}$, $p_h$ is the hydrostatic component of the pressure, and $p_{hs}$ and $p_{ht}$ refer to values along the surface and top boundaries, respectively. The coordinate definition in (1), proposed by Laprise (1992), is the traditional $\sigma$ coordinate used in many hydrostatic atmospheric models. This vertical coordinate is also called a mass vertical coordinate. The model equations are written in flux form. Spatial discretization uses Arakawa C-grid staggering for the model variables. The model integration uses time-split third-order Runge–Kutta scheme with smaller time step for acoustic and gravity wave modes. More detailed description of the WRF model with dry dynamical core can be found in Skamarock et al. (2005).

We started with a basic, adiabatic version for the tangent linear and adjoint model development. It excludes all major model physics (e.g., the parameterizations for cumulus, microphysics, and radiation). However, both horizontal and vertical diffusions are retained in the adiabatic model. To include a very simple boundary layer process, a surface drag scheme that is similar to Buizza (1994) is incorporated into the model. The scheme essentially provides the model with a surface friction stress that is distributed over the lowest few levels with a linearly decreasing weight. The surface drag coefficient ($C_d$) simply depends upon whether it is over land or water. For land, $C_d = 0.01$. Over water, $C_d = 0.0001V$ for low-level wind ($V$) greater than 10 m s$^{-1}$, and $C_d = 0.001$ for weaker winds. For coastal points we assign $C_d = 0.003$. The surface friction stress is then distributed through the lowest levels (up to height $H$). The tendency terms due to surface stress at height $z$ are

$$\frac{\partial u}{\partial t} = -W(z)\tau_x/H \quad \text{and}$$
$$\frac{\partial v}{\partial t} = -W(z)\tau_y/H, \tag{2}$$

where $\tau_x$ and $\tau_y$ are the surface friction stress components in $x$ and $y$ directions, respectively, and the vertical weight $W(z)$ is given by

$$W(z) = \begin{cases} 2\dfrac{H - z}{H}, & (Z < H) \\ 0, & (Z > H) \end{cases}. \tag{3}$$

### b. Tangent linear model and its adjoint

We used TAF to generate the tangent linear and adjoint models for the adiabatic WRF model. Because of the complexity of the model, not all generated codes were correct. TAF had difficulty in handling the WRF model integration scheme (third-order Runge–Kutta large time steps and small acoustic time steps). It also generated a lot of unnecessary basic-state recalculations for the adjoint perturbations. We had to conduct a correctness verification for each subroutine and the top-level solver routine. We made efforts to remove some of the unnecessary recalculation in the adjoint code. The correctness verification was always conducted every time we made a reduction of recalculation and bug fix. The so-called tangent linear and adjoint check procedure follows that of Thépaut and Courtier (1991) and Navon et al. (1992).

We performed the tangent linear and adjoint checks by integrating the WRF-ARW for one time step, several hours, and up to 24 h. The AMPS initial and boundary conditions of 90-km resolution domain (Fig. 1a) were used for the integration. The initial and boundary conditions were interpolated from the NCEP GFS analysis. The surface wind and SLP at 0000 UTC 15 May 2004 are shown in Fig. 3. To ensure the correctness of the developed tangent linear and adjoint, verifications with a lot of different cases should be conducted. But for this severe wind case, both the tangent linear and adjoint codes of the adiabatic WRF model passed the correctness check. The testing was performed on the NCAR IBM machine with 64-bit precision. The tangent linear and adjoint codes of the WRF simplified model were verified within machine accuracy (Navon et al. 1992).

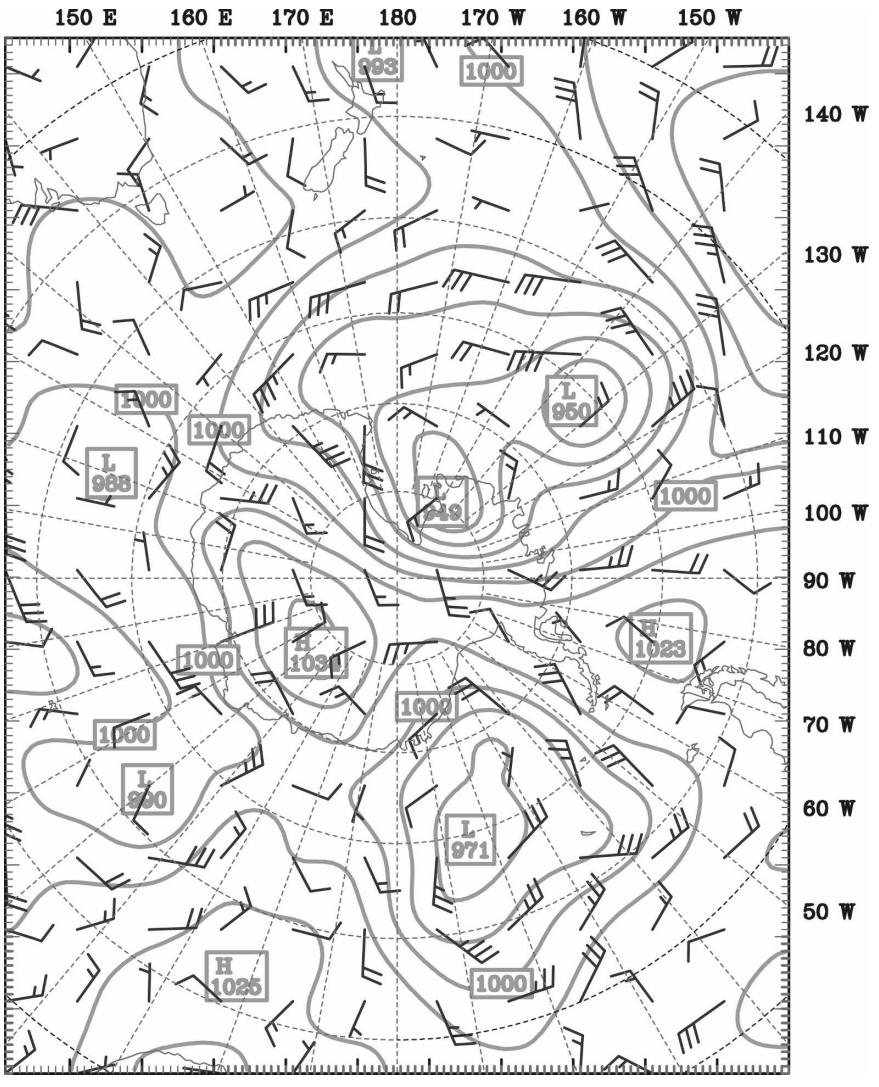


FIG. 3. The surface wind and SLP (gray isolines) at 0000 UTC 15 May 2004, interpolated from the NCEP GFS analyses. The domain is the same as the domain 1 shown in Fig. 1a. A full wind barb represents 5 m $s^{-1}$ and the interval of SLP isolines is 5 hPa.

## 4. WRF control simulations and linearity test

With the initial conditions in Fig. 3 for a 90-km resolution AMPS domain in Fig. 1a, WRF control experiments were conducted. The domain configuration is the same as AMPS domain 1 for the real-time setup. There are 110 × 145 grid points in the horizontal and 32 levels in the vertical direction.

### *a. Control simulation with the WRF full-physics model*

The first control experiment includes a full-physics package in the WRF model. The physics used include WSM six-class graupel microphysics scheme, a rapid radiative transfer model for the longwave radiation (Mlawer et al. 1997), Dudhia's (1989) shortwave radiation scheme, the Yonsei State University planetary boundary layer scheme (Hong et al. 2006), and the Betts–Miller cumulus parameterization scheme. The 24-h forecast of surface winds and sea level pressure (Fig. 4a) shows that the cyclone moves to Victoria Land to the north of the Ross Island at 0000 UTC 16 May 2004.

### *b. Control simulation with the adiabatic WRF model*

The adiabatic WRF model was used for the development of the WRF tangent linear and adjoint models. It

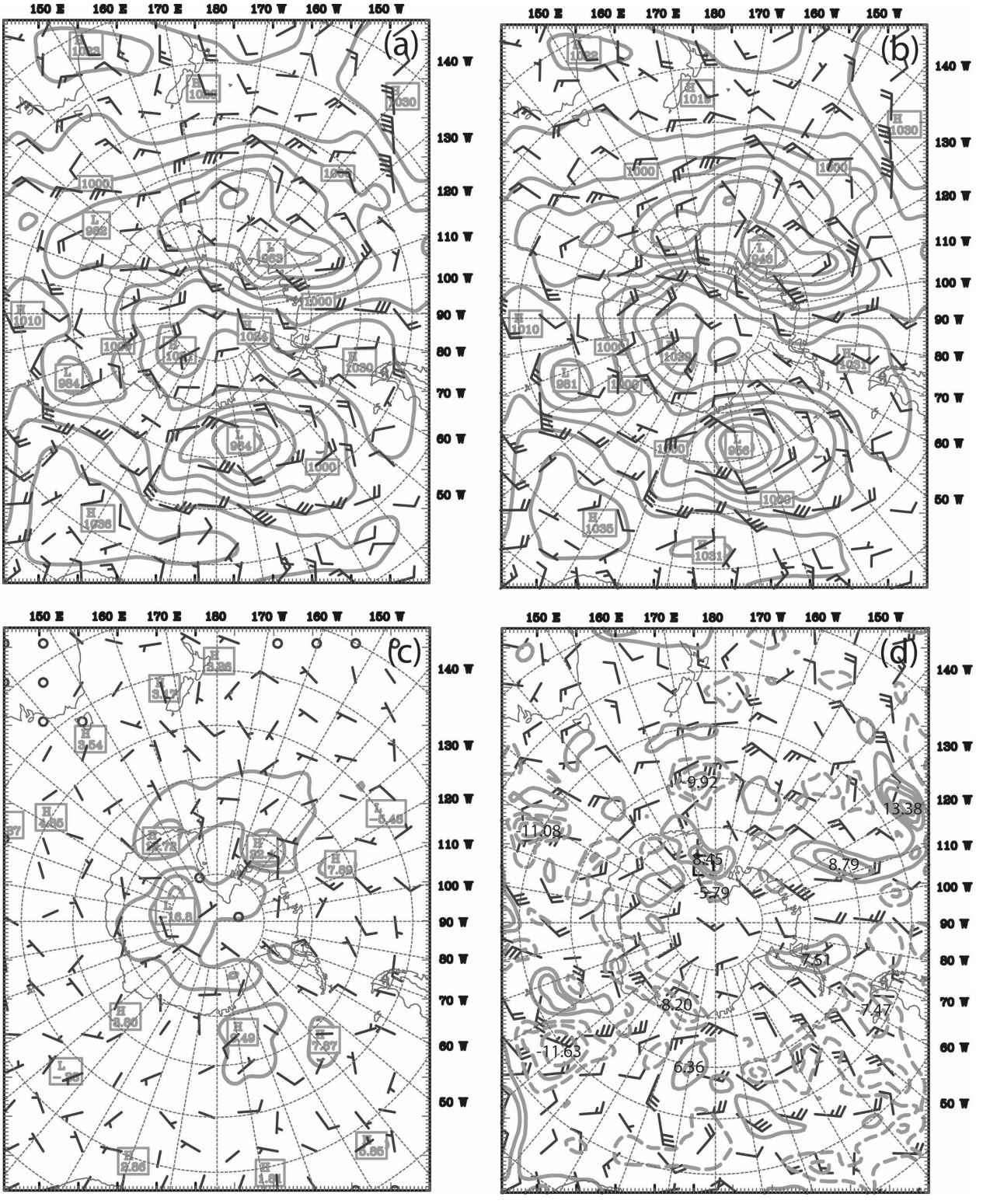


FIG. 4. The 24-h forecasts of the surface winds (barbs) and SLP (gray isolines, 10-hPa interval) at 0000 UTC 16 May 2004 by (a) the WRF full-physics model and (b) the adiabatic version of WRF model. (c) The difference fields between full-physics and adiabatic model forecasts at 24 h. (d) The NCEP GFS analysis of surface winds (barbs) and the difference of surface wind speeds (isolines, 3 m $s^{-1}$ interval) between the adiabatic forecast and NCEP GFS analysis at 0000 UTC 16 May. The sensitivity response box is shown in (d). A full barb represents 5 m $s^{-1}$.

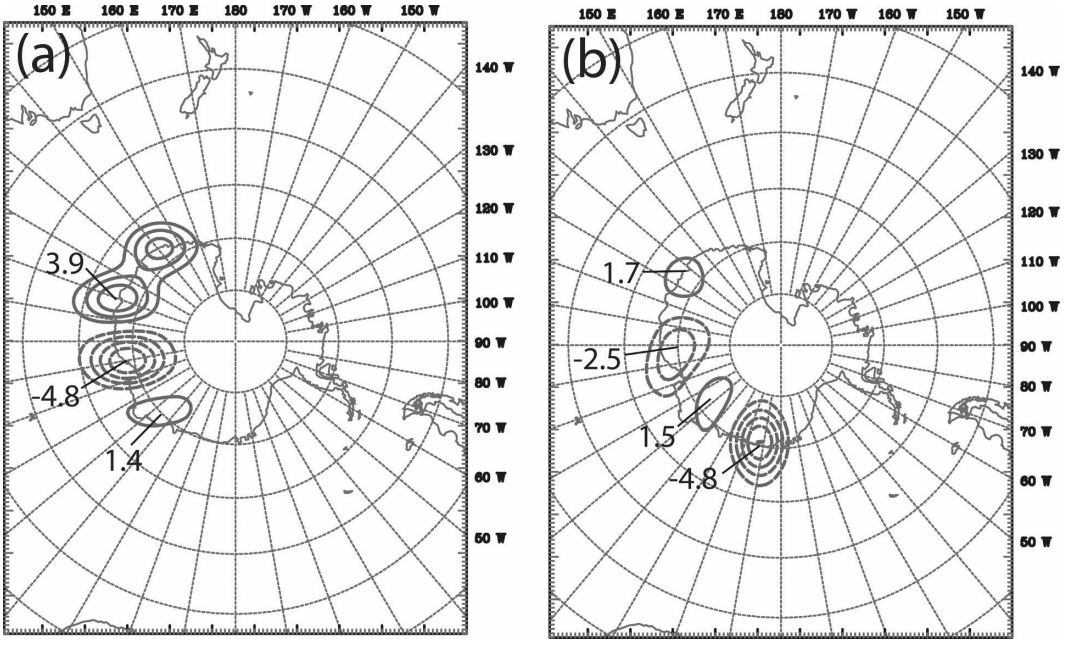


FIG. 5. Initial perturbations of surface wind components (WRF 3DVAR increments by assimilating 8 radiosonde station data in Antarctica) at 0000 UTC 15 May 2004: (a) $\delta u$ and (b) $\delta v$. The intervals of the isolines for $\delta u$ and $\delta v$ are 1 m s$^{-1}$ and the zero line is omitted.

excludes all the model physics and only simple diffusion and surface drag are included. To compare the forecasts between the WRF full-physics and adiabatic models, a control experiment using adiabatic WRF was conducted. The 24-h forecast of surface winds and sea level pressure is shown in Fig. 4b. Similar to the forecast from the WRF full-physics model, the cyclone is predicted to move to Victoria Land area at 0000 UTC 16 May. The adiabatic model with vertical diffusion and surface drag produced similar wind distribution and speed in Ross Sea, compared with the full-physics model. The major synoptic patterns in surface wind and SLP distributions of the 24-h forecasts are similar in both the full-physics and adiabatic experiments (Figs. 4a,b).

Figure 4c shows the difference fields of the surface wind and SLP between Figs. 4a,b. The surface wind differences are between 0 and 8 m s$^{-1}$. With model physics included, the WRF full-physics model produced weaker cyclone intensity than its adiabatic version did. Because the SLP low/highs are shifted, their SLP intensities show larger differences in Fig. 4c. The surface wind at McMurdo is about 2 m s$^{-1}$ stronger in the adiabatic model run (10 m s$^{-1}$) than in the full-physics model run (8 m s$^{-1}$). Both underpredicted the surface wind at McMurdo at 0000 UTC 16 May 2004 (28.9 m s$^{-1}$ in observation). Figure 4d shows the National Centers for Environmental Prediction (NCEP) analysis of surface wind, and the differences between the adiabatic forecast and the analysis at 0000 UTC 16 May. In the McMurdo area, the surface wind speeds of the NCEP analysis are around 5 m s$^{-1}$ smaller than in the adiabatic forecast. Because most of the facilities were damaged by the windstorm before 0000 UTC 16 and the observational records were truncated, the NCEP analysis did not show strong winds at the 0000 UTC 16 analysis time. The 24-h forecast by the adiabatic model improves the windstorm intensity from the NCEP GFS analysis. The adiabatic WRF adjoint is used in this study for an adjoint sensitivity analysis. This event was mainly a dynamic process, and the Antarctic terrain played an important role in the severe wind. The adiabatic WRF adjoint is suitable for this adjoint sensitivity study. However, inclusion of model physics should be considered as a next step for the WRF tangent linear and adjoint models.

### c. *Linearity test*

In addition to evaluating the performance of the control simulations, it is necessary to assess the validity of the tangent linear assumption prior to discussing any adjoint-based results (Vukicevic 1991; Errico and Vukicevic 1992; Gilmour et al. 2001). Figure 5 shows examples of the initial perturbations of wind components at the surface used for performing the 24-h linearity test. The perturbations are, in fact, the WRF

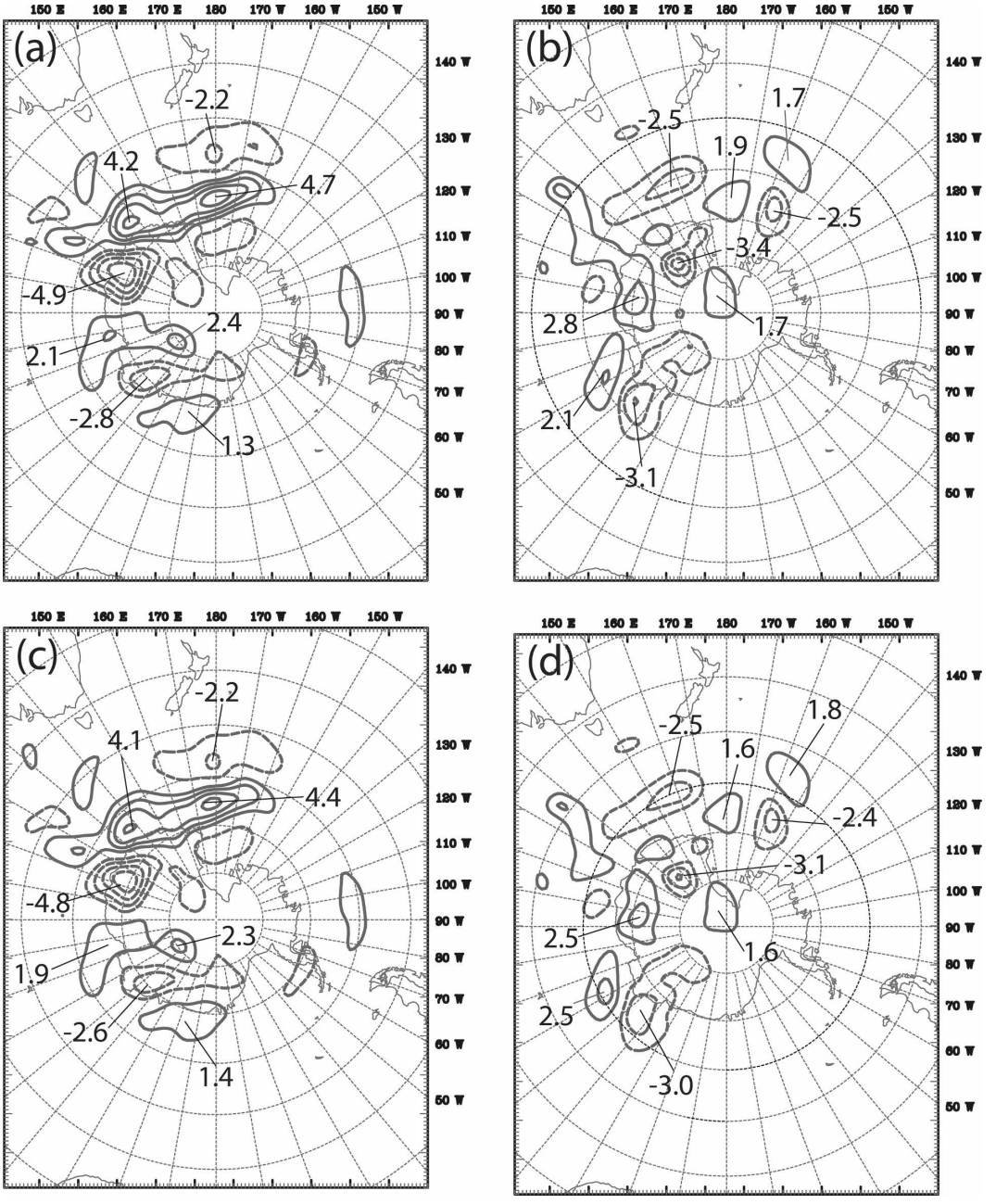


FIG. 6. The difference of (a) $u$ component and (b) $v$ component of the surface wind between two parallel adiabatic WRF model runs, and (c) $u$ increment and (d) $v$ increment of the surface wind by WRF tangent linear model integration at 0000 UTC 16 May 2004 (24-h forecast). The interval of the isolines is 1 m s$^{-1}$ and the zero line is omitted.

three-dimensional variational data assimilation (3DVAR) increments by assimilating eight radiosonde soundings in Antarctica at 0000 UTC 15 May 2004. Two parallel nonlinear forecasts using the adiabatic model are conducted: one without the initial perturbations and the other with the increments added to the initial conditions. The forecast differences of the two parallel runs can evaluate the nonlinear evolution of the perturbations (Figs. 6a,b). Meanwhile, we applied the initial perturbations to the WRF tangent linear model, and the results of the WRF tangent linear model integration were used to analyze the linear evolution of the perturbations (Figs. 6c,d).

The differences of two nonlinear integrations (Figs.

TABLE 1. Ratio of norms ($R$) between the tangent linear forecasts and the differences of the two nonlinear model forecasts at 24 h. The norm is defined as the summation of the squares of all variables (perturbations of tangent linear model and difference of two nonlinear models) over the whole domain at 24 h. Here $\alpha$ is the decreasing factor of the initial perturbations $\mathbf{X}'$, as shown in Fig. 5.

| $\alpha$ | $R$ |
|---|---|
| 1 | 0.103 852 905 897 9 |
| $10^{-1}$ | 0.101 289 746 434 7 |
| $10^{-2}$ | 0.100 341 782 776 7 |
| $10^{-3}$ | 0.100 072 490 290 9 |
| $10^{-4}$ | 0.100 002 814 941 1 |

6a,b) are very similar to the tangent linear solutions displayed in Figs. 6c,d. The pattern similarity between the linear and nonlinear solutions is obvious even though their amplitudes are slightly different. The comparison reveals that the linearly evolved perturbation and nonlinear difference have qualitative and quantitative agreement (Fig. 6). As further validations, we sequentially reduced the initial perturbations by a factor of $10^{-1}$ and repeated the above experiments. Table 1 shows the ratios of norms between the 24-h tangent linear forecasts and the differences of two nonlinear forecasts over the whole domain. The norm in the table is defined as the summation of the squares of all variables (perturbations of tangent linear model and difference of two nonlinear models) over the whole domain at 24 h. It indicated that the tangent linear forecast approximates the difference of two nonlinear forecasts as the initial perturbations decrease and approach zero.

These results demonstrate that the perturbation evolution is well represented by the WRF tangent linear solutions up to at least 24 h for the 90-km resolution domain at high southern latitudes. In this test, the basic-state trajectory of the WRF tangent linear model is updated every time step from the adiabatic WRF model in this study. The linearity test provides useful information for the WRF four-dimensional variational data assimilation (4DVAR) setup, especially for the 4DVAR assimilation time window configuration (Xiao et al. 2000, 2002). It also suggests that the adjoint sensitivity of the 24-h forecast for this case is valid.

## 5. Adjoint sensitivity analysis of the May 2004 McMurdo windstorm with WAMS

### *a. Definition of the response function*

The adjoint technique is a computationally efficient method to determine the sensitivity of a forecast's response to model initial conditions (Errico and Vukicevic 1992; Zou et al. 1993; Li et al. 1999; Xiao et al. 2002). It can be used to locate high-sensitivity regions where small perturbations can have relatively large effects on forecast features. The goal of a sensitivity study is to estimate how a particular differentiable function of the model forecast state (called a response function, $R$) defined at a specific forecast time ($t_f$) can be modified by changing the model initial state ($\mathbf{X}^0$). This estimate, $\delta R$, is obtained by evaluating the inner product of a sensitivity gradient ($\partial R/\partial \mathbf{X}^0$, the gradient of $R$ with respect to the model state at initial time) with a contemporaneous model initial perturbation ($\delta \mathbf{X}^0$):

$$\delta R = \left\langle \frac{\partial R}{\partial \mathbf{X}^0}, \delta \mathbf{X}^0 \right\rangle. \tag{4}$$

The adjoint of an NWP model is the most efficient means of calculating the required sensitivity gradient (Errico 1997). Figure 7 shows the schematic of the flowchart for calculating the adjoint sensitivity. Once the response function is defined at the forecast time $t_f$, the forcing of the adjoint model, $\partial R/\partial \mathbf{X}^f$, is then calculated as one of the initial conditions for the backward integration. Another required input is the basic-state trajectory, which is stored during the nonlinear model integration. In this study, we stored the trajectory at every time step.

The definition of response function, $R$, is usually selected according to the problem to be explored. In Gustafsson and Huang (1996), forecast error, defined as the difference between forecast and verifying analysis using energy norm, is chosen as $R$. Considering the McMurdo windstorm in this study, we define the response function as half of the square of the forecast wind speed at 0000 UTC 16 May 2004 in the rectangular box (Figs. 4 and 8) around the McMurdo Station:

$$R = \frac{1}{2} \sum_{i,j} [(u^f_{i,j})^2 + (v^f_{i,j})^2], \tag{5}$$

where $(u^f_{i,j}, v^f_{i,j})$ are the WRF forecast surface wind components on the WRF grid points $(i, j)$ inside the response box at 0000 UTC 16 May 2004. It is obvious that the value of $R$ represents the intensity of the forecast windstorm around McMurdo Station. With the WRF adjoint model integration, the gradient of the defined response function (adjoint sensitivity) can be calculated. If we define the adjoint integration back to initial time as

$$\frac{\partial R}{\partial \mathbf{X}^0} = L^* \frac{\partial R}{\partial \mathbf{X}^f}, \tag{6}$$

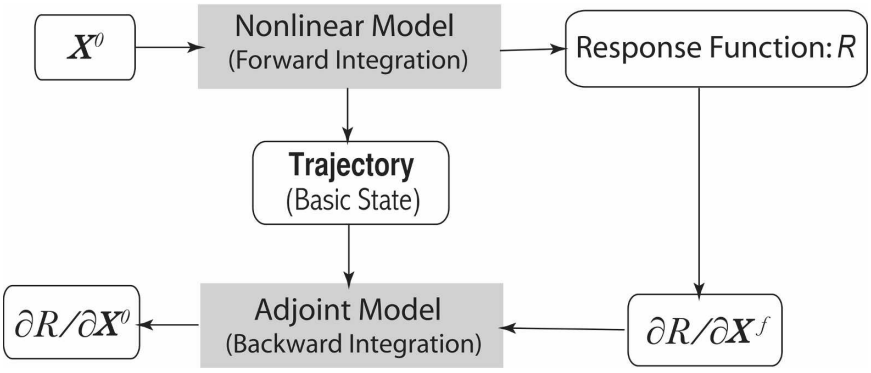


FIG. 7. Schematic outlining the flowchart of adjoint sensitivity calculation.

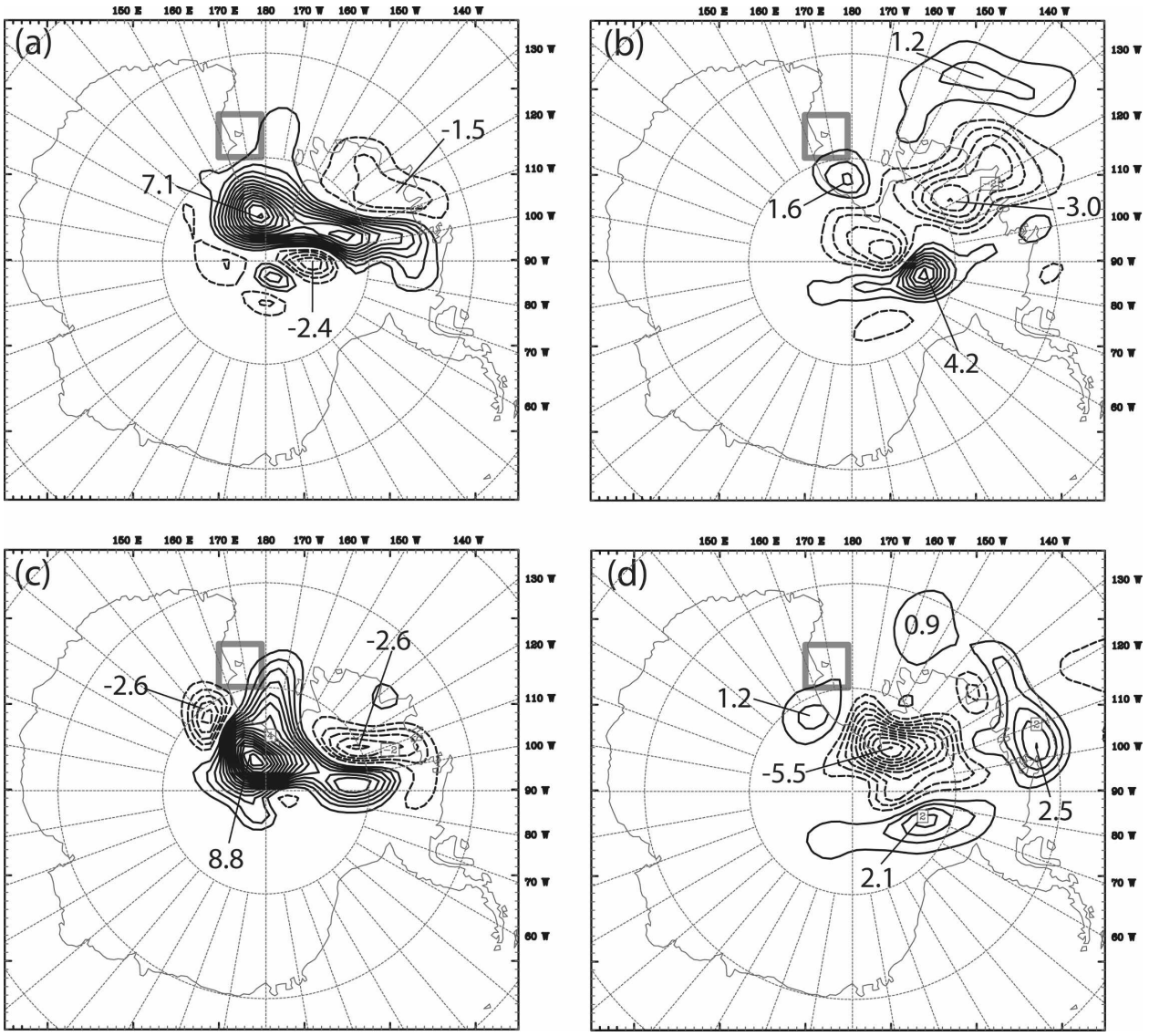


FIG. 8. Sensitivity of the windstorm intensity $R$ in the McMurdo area (the black box shown in the figures) with respect to $u$ at (a) $\sigma = 0.9965$ (layer 31) and (b) $\sigma = 0.7565$ (layer 17), and to $v$ at (c) $\sigma = 0.9965$ (layer 31) and (d) $\sigma = 0.7565$ (layer 17). The intervals of the gradients of $u$ and $v$ are both 0.5 m s$^{-1}$. Negative contours are dashed.

the adjoint sensitivity is calculated according to (4) as

$$\delta R = \left\langle L^* \frac{\partial R}{\partial \mathbf{X}^l}, \delta \mathbf{X}^0 \right\rangle. \quad (7)$$

Therefore, the output of the adjoint model is the gradient of a response function with respect to the model initial conditions, and can be utilized to estimate the change in the value of that response function associated with any arbitrary, but small, perturbation to the model input. Note, that in contrast to the nonlinear and linearized models that relate model input to model output, the adjoint model maps the gradient of the response function with respect to the model output to the gradient of the response function to the model input. The adjoint of an NWP model is integrated "backward" in time to obtain the gradient of a response function with respect to the model state at initial time. Based on the definition of the response function of (5), the only nonzero gradients for the adjoint model input are with respect to the horizontal wind components inside the defined box shown in Fig. 8.

### b. *The adjoint sensitivity for 24-h forecast of the storm*

For the selected windstorm case on 15 May 2004, we carried out an adjoint sensitivity examination for the initial conditions (0000 UTC 15 May 2004), as determined by a backward integration of the adiabatic WRF adjoint over a 24-h period. If an initial condition in the positively sensitive area is increased, the predicted windstorm will be stronger and vice versa for the negatively sensitive area. This assertion holds under the assumption that the linear approximation is valid. As we verified in the last section, the linearity of the WRF tangent linear and adjoint model for 24-h forecast of the Antarctica case is valid.

Figure 8 shows the sensitivity gradient distribution of the predicted windstorm intensity in McMurdo area at 0000 UTC 16 May 2004 with respect to the initial wind components ($u$ and $v$) at 0000 UTC 15 May (initial time). For the 24-h forecast of the windstorm in the McMurdo area (the box in Fig. 8), the initial winds at 0000 UTC 15 May are sensitive to its intensity. In other words, the initial winds (magnitude and distribution) have a significant contribution to the formation and strength of the McMurdo windstorm. Figure 8 indicates that the adjoint sensitivity with respect to the initial wind fields has a different pattern in the lower levels than in the midlevels. At $\sigma = 0.9965$, the sensitivity to winds in the initial analyses is located in the area south of the Ross Ice Shelf near the South Pole extending to West Antarctica (Figs. 8a,c). The sensitivities to $u$ are mostly positive in the area, with only a small negative sensitivity area along the 90°W line in West Antarctica and in Marie Byrd Land (Fig. 8a). The sensitivities to $v$ are positive in the area near the South Pole, with negative sensitivities aside in East Antarctica and Marie Byrd Land in West Antarctica, respectively (Fig. 8c). At the layer 17 ($\sigma = 0.7565$; Figs. 8b,d), the sensitivity to initial winds in the Antarctic area are opposite in sign to that at lower levels. In the area to the south of Ross Ice Shelf from the East Antarctica to West Antarctica where the sensitivity gradients are positive (Figs. 8a,c), we would need to increase $u$ and $v$ for a intense windstorm prediction in McMurdo. Likewise, we would need to decrease $u$ and $v$ at the midlevels ($\sigma = 0.7565$) in the area south of the Ross Ice Shelf extending to the Marie Byrd Land in the West Antarctica (Figs. 8b,d). In other words, the southerly or southwesterly winds at lower levels in the south edge of Ross Ice Shelf to West Antarctica should increase and the northeasterly wind at midlevels from the South Pole to Marie Byrd Land should increase, so as to improve the windstorm prediction (in this case, to increase the intensity of the windstorm at 0000 UTC 16 May 2004). It must be pointed out that the required changes in initial conditions are purely from adjoint sensitivity analysis. Because the adjoint model was developed from an adiabatic version of WRF, we could not include contributions of model physics to the severe wind prediction. However, such a severe wind event is mainly an adiabatic process where terrain plays a major role (discussed in section 5c). The adjoint sensitivity analysis from adiabatic adjoint model should provide a good indication of the full-physics model forecast. We will verify the results in the next section.

Rather than displaying the sensitivities with respect to horizontal wind components as separate scalar fields, an alternate way is to show sensitivity vector as defined by Kleist and Morgan (2005a). The advantage of the representation of sensitivity vector is that greater insight is afforded into the relative magnitude and directions of the required perturbation to the wind field to get maximum changes in a given response function. Figure 9a indicates that the sensitivity vectors at $\sigma = 0.9965$ in the area between Ross Ice Shelf and South Pole along 180° are toward the north or northeast. But at the midlayers such as at $\sigma = 0.7565$ (Fig. 9b), the sensitivity vectors are toward southwest direction in the area as well as in Marie Byrd Land in West Antarctica. This means that one should increase the south or southwest winds in the area between Ross Ice Shelf and South Pole at lower levels and decrease them from Marie Byrd Land to South Pole, in order to have a

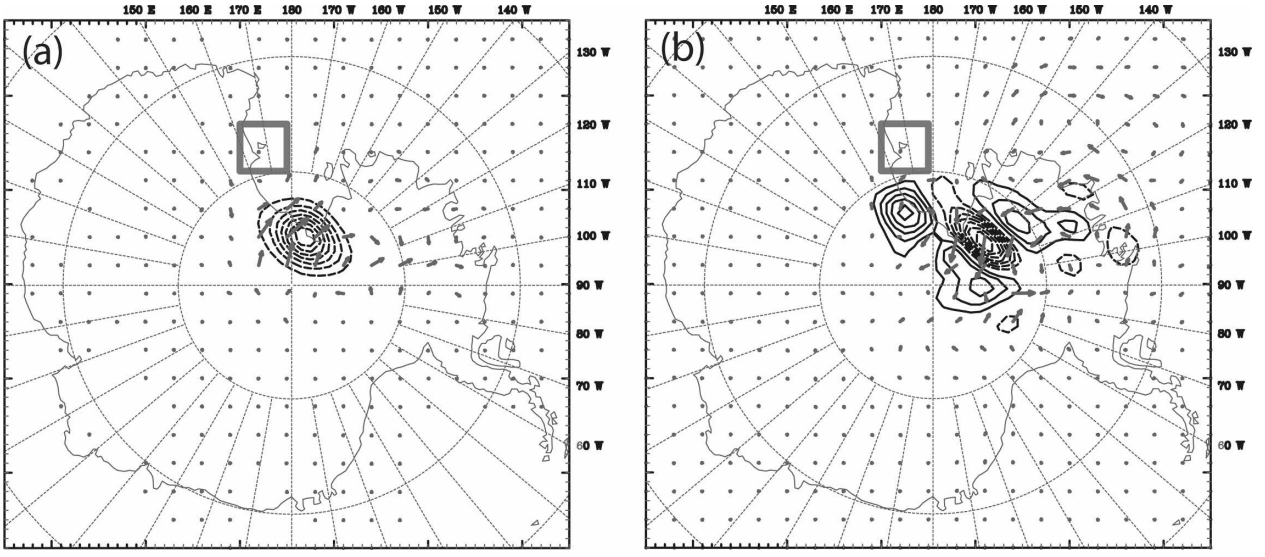


FIG. 9. Sensitivity of the windstorm intensity $R$ in the McMurdo area (the black box shown in the figures) with respect to pressure at (a) $\sigma = 0.9965$ (layer 31) and (b) $\sigma = 0.7565$ (layer 17). The intervals of pressure gradients are 0.0001 $m^2\,s^{-2}\,hPa^{-1}$ for (a) and 0.000 000 5 $m^2\,s^{-2}\,hPa^{-1}$ for (b). Also plotted are sensitivity vectors ($m\,s^{-1}$).

more intense windstorm (closer to the real observation) in the McMurdo Station.

Also shown in Fig. 9 are the sensitivities of the McMurdo windstorm to pressure at lower level ($\sigma = 0.9965$; Fig. 9a) and midlevel ($\sigma = 0.7565$; Fig. 9b). It indicates that the rather weak windstorm prediction is also due to higher pressure at the lower levels in the area south of the Ross Ice Shelf and north of the South Pole (Fig. 9a). At midlevel (Fig. 9b), the pressure should deepen in the area between Ross Ice Shelf and Marie Byrd Land. According to the sensitivity analysis, the pressure low should be located farther southeast from the analysis so as to increase the intensity of the predicted McMurdo windstorm.

Figure 10 is the calculated gradient distribution of the predicted windstorm intensity in the McMurdo area at 0000 UTC 16 May 2004 with respect to the initial potential temperature ($\theta$) at 0000 UTC 15 May (initial time). A very sensitive (negative gradient) area to potential temperature is shown along the international date line between the Ross Ice Shelf and the South Pole at the lowest layer $\sigma = 0.9965$ (Fig. 10a) in the initial analysis at 0000 UTC 15 May. The negatively sensitive area is circular and the most sensitive (minimum value) location is in the high land south of the Ross Ice Shelf. In the circular area the winds are southerly or south-southeasterly from the South Pole to Ross Island. The negative sensitivity in the area indicates that the value of the lower-level temperature (or potential temperature) in the analysis should be decreased in order to have a stronger windstorm prediction 24 h later. We found that negative sensitivities are limited to the lowest several levels. At higher levels, the sensitivity pattern is different. As indicated in the cross section of the potential temperature gradient (Fig. 10b), negative gradients are located in the boundary layer of the high land and at high levels above the South Pole area. Over the Ross Ice Shelf are positive gradients from lower to high levels. There are also positive sensitivities shown across the South Pole at the lower levels. On the downward slope of the high land to Ross Ice Shelf, the adjoint sensitivity gradient of the potential temperature indicates that the boundary layer near the downward slope surface should have reduced the temperature while upper levels should have increased the temperature. The atmospheric stability (stratification) should be increased on the downward slope to Ross Ice Shelf in order to increase the McMurdo windstorm intensity prediction 24 h later.

### c. *Physical meanings behind the distribution of the calculated adjoint sensitivity*

Described in sections 4a and 4b, the control simulations using both the full-physics model and its adiabatic version did not produce as strong a windstorm as observed in the McMurdo area. Powers (2007) indicated that appropriate initial conditions enhanced by the Moderate Resolution Imaging Spectroradiometer (MODIS) wind data assimilation could improve the storm forecast. In this study, the adjoint sensitivity analysis also provides insightful indication that the shortcomings in the initial conditions contribute a great

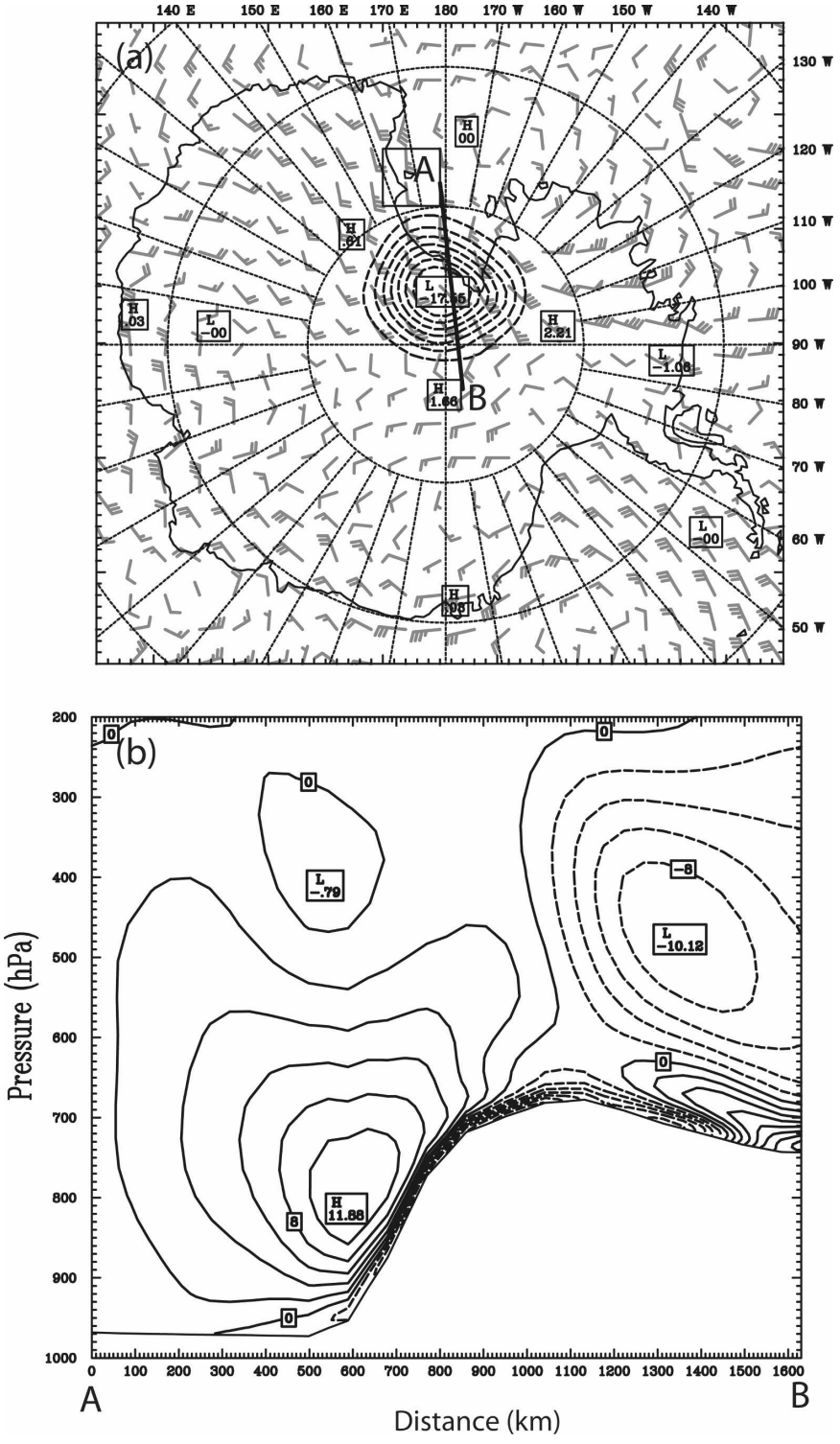


FIG. 10. Sensitivity of the windstorm intensity $R$ in the McMurdo area (the black box shown in Fig. 11a) with respect to temperature: (a) the lower level $\sigma = 0.9965$ (the wind barbs are overlapped) and (b) cross sections along AB shown in (a). The intervals of temperature gradients are 2 $m^2 s^{-2} K^{-1}$ and a full barb represents 5 $m s^{-1}$ wind.

deal to the failure of the windstorm prediction at 0000 UTC 16 May 2004.

The analysis shows that the wind flows at the lowest model level (Fig. 10a) are most southerly or south-southeasterly from the South Pole and West Antarctica area through Ross Ice Shelf to the McMurdo area in the Ross Sea. The topography over the flow passage area is special, having high land over the South Pole and West Antarctica, and being flat over the Ross Ice Shelf and Ross Sea (see Fig. 10b). Studies by Bromwich et al. (1992) and Bromwich et al. (1994) indicate that the terrain in the area is prone to katabatic winds over the Ross Ice Shelf and McMurdo area. The katabatic winds over the Ross Ice Shelf and McMurdo region are the results when the air over the Antarctic high land becomes negatively buoyant and accelerates downslope onto the Ross Ice Shelf and Ross Sea (Bromwich 1989). At 0000 UTC 15 May, the cyclone is over West Antarctica; the west sections of the cyclone (around the international date line) are influenced by southerly or south-southeasterly winds. Figures 8 and 9 suggest that the southerly winds over the Antarctic high land in the analysis should be increased at lower levels, but at high levels there should be increased northeasterly winds at the Siple Coast and West Antarctica. This is to increase the inflow speed of the downslope wind at lower levels and its shear in the vertical above the high land of Antarctica. The current analysis in the area has the wind speed lower than the adjoint sensitivity indicated. Another obvious feature shown in Fig. 10b, is that the temperature (potential temperature) above the Antarctic high land and its north slope should be colder than the analysis in the lower levels. The stratification over the north slope of the Trans-Antarctic Mountains should be more stable than the analysis (i.e., $\partial\theta/\partial z$ should be larger over the north slope).

The Froude number ($F_r$) is often used as a parameter to describe the stratification of the atmosphere in relation to the airflow to study flow over mountains or downward of the mountains. According to Burk et al. (1999), the Froude number is defined as

$$F_r = U\left(gH\frac{\Delta\theta}{\theta}\right)^{-1/2}, \tag{8}$$

where $U$ is the wind speed, $g$ is the gravitational acceleration (9.8 m s$^{-2}$), $H$ is the height of the mountain, $\Delta\theta$ is the increase of potential temperature between the Ross Ice Shelf and the top of the high land, and $\theta$ is the average potential temperature of the layer between the Ross Ice Shelf and the top of the high land. Based on the adjoint sensitivity analysis, $U$ should increase (Figs. 8 and 9), and $\Delta\theta$ between the Ross Ice Shelf and the top of the high land should be decreased. In other words, the Froude number ($F_r$) should be much larger in the real atmosphere than the analysis. In the following section, we will verify the assertion by assimilating some pseudo-observations that are constructed based on the adjoint sensitivity information of wind and temperature in the area to see if the McMurdo windstorm can be intensified from the control simulations.

## 6. Numerical experiments of the windstorm using sensitivity gradient information

Although the adiabatic WRF adjoint is used, the described sensitivity gradient (the wind speed change around the McMurdo Station with respect to the model initial state) may be used to identify the sensitive regions and variables that specifically contribute to $R$ in (5). Modifying the analysis using the gradient information can lead to an increase of the wind speed around McMurdo as measured by $R$ of (5). As a simple test, we selected 14 grid points as shown in Fig. 11, and made pseudo-observations. The perturbations of 5 m s$^{-1}$ in wind components ($u$, $v$) and 5 K in temperature ($T$) of the same sign as the sensitivity fields are projected onto the pseudo-observations. Using the WRF 3DVAR, these 14 pseudo-observations plus the conventional data were assimilated. In the following, we will compare the forecasts of the windstorm using the full-physics WRF model from 4 experiments: CTRL (the initial conditions are AMPS analyses), GTS (the CTRL analyses are enhanced by conventional GTS data), GTSUV (the CTRL analyses are enhanced by conventional GTS data plus winds of the 14 pseudo-observations), and GTSUVT (the CTRL analyses are enhanced by conventional GTS data plus winds and temperature of the 14 pseudo-observations). In the 3DVAR experiments, the National Meteorological Center method (Parrish and Derber 1992) was used to conduct the background error statistics. The differences between 24- and 12-h AMPS forecasts in May 2004 were taken as background errors to calculate the background error covariance. The observational errors for conventional data were from NCEP, and the errors of pseudo-observations were the same as radiosonde observation errors. As expected, the increments of wind and temperature with the pseudo-observations are much smaller than 5 m s$^{-1}$ and 5 K, respectively. However, small perturbations in the initial conditions in the sensitivity area would experience rapid growth in the forecast. We will analyze the 24-h forecast of the experiments with pseudo-observations in the following.

First of all, assimilation of the limited GTS observa-

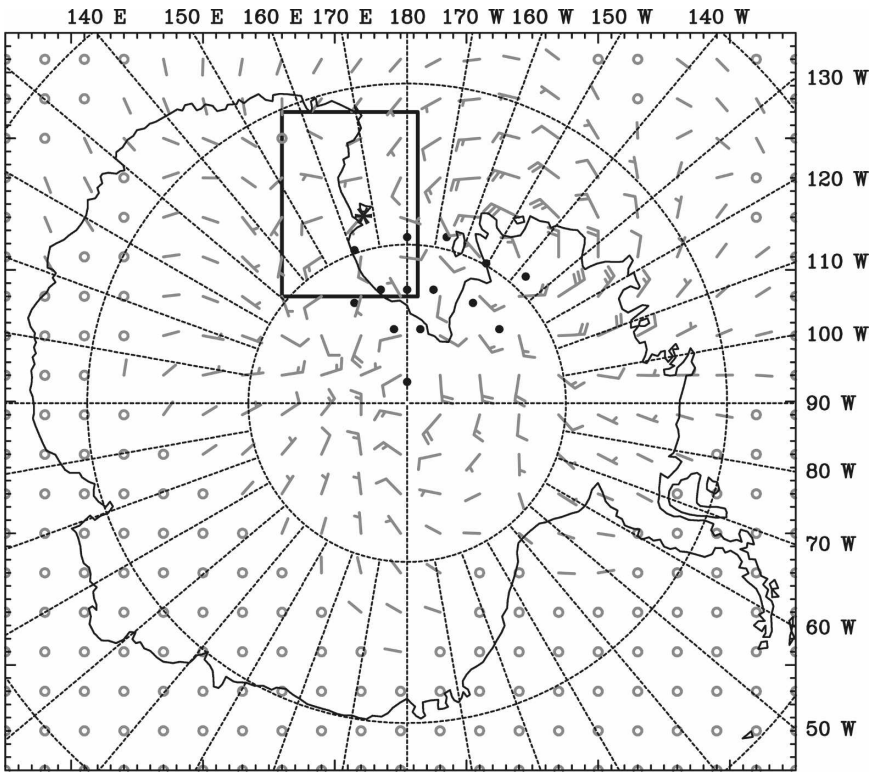


FIG. 11. Locations of the 14 pseudo-observations (black dots) and the wind difference barbs between GTSUV and GTS at the lower level $\sigma = 0.9965$. A full barb represents 5 m s$^{-1}$. McMurdo Station is shown with an asterisk. The black box is the domain for the forecasts shown in Fig. 12.

tions in Antarctica slightly improved the McMurdo severe wind forecast. The 24-h surface wind forecast at McMurdo is about 8 m s$^{-1}$ in CTRL; but GTS predicted about 10 m s$^{-1}$. If we had observations in the sensitive region, the McMurdo severe wind event would be better predicted. This assertion can be verified by comparing the analysis increments of GTSUV and GTSUVT from GTS. In GTSUV and GTSUVT, the model initial conditions are enhanced by the pseudo-observations that are constructed based on the adjoint gradient information. Figure 11 shows an example of the impact from pseudowind observations (in experiment GTSUV) compared with GTS. The southeasterly winds at the Siple Coast and West Antarctica are increased at the lowest level in experiment GTSUV after assimilating the pseudo-observations. The southwesterly winds on the north slope of the Trans-Antarctic Mountains are also increased in experiment GTSUV. These wind changes are based on the adjoint sensitivity information, but the influence on the forecast of the McMurdo windstorm is large (Fig. 12). It verifies that the forecast of the windstorm is sensitive to the model initial conditions in the area.

The comparison among Figs. 12a–d demonstrates that the surface winds at McMurdo area by the experiments with the assimilation of adjoint sensitivity pseudo-observations (GTSUV and GTSUVT) are much increased from the experiments that did not assimilate the adjoint sensitivity pseudo-observations (CTRL and GTS). Note that assimilating the limited conventional GTS data in Antarctica is not enough to enhance the analysis for the severe storm prediction (Fig. 12b), albeit it does change the forecast wind distribution around McMurdo (cf. Figs. 12a,b). The GTS experiment obtains about 2 m s$^{-1}$ increase of the wind prediction at McMurdo Station over CTRL. With the assimilation of pseudo-observations, the forecast wind speed in McMurdo is greatly increased. GTSUV obtains 19 m s$^{-1}$ and GTSUVT has 25 m s$^{-1}$ in McMurdo at 0000 UTC 16 May. When compared with the observation of 28.9 m s$^{-1}$ surface wind, GTSUVT has a better forecast of the windstorm intensity than GTSUV. It illustrates that temperature modifications from the sensitivity information play as important a role as wind modifications. Using the adjoint sensitivity information in both wind and temperature pseudo-

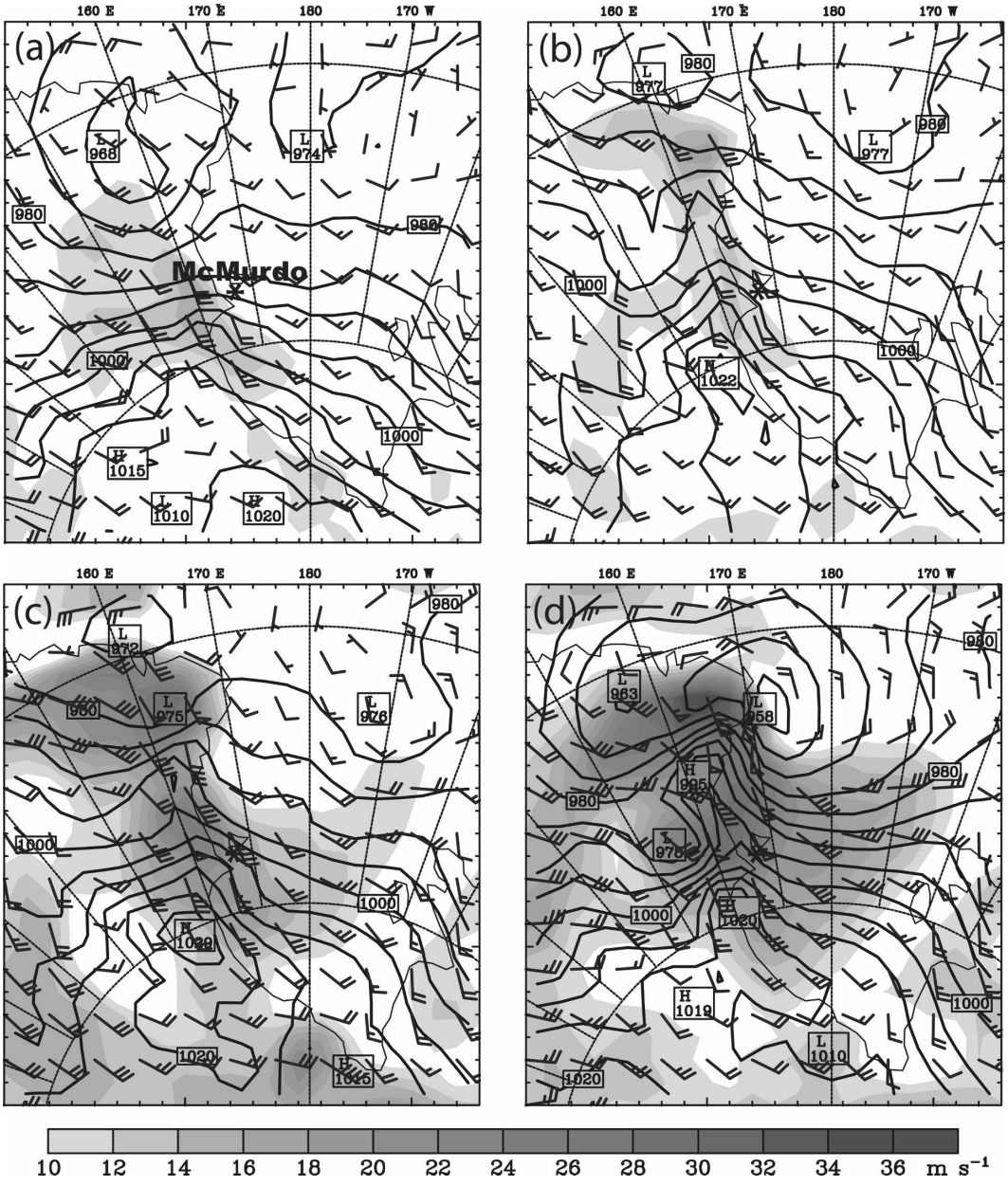


FIG. 12. The 24-h forecasts of the surface winds and SLP (hPa) at 0000 UTC 16 May 2004 from experiments (a) CTRL, (b) GTS, (c) GTSUV, and (d) GTSUVT. The figures are for the black box area shown in Fig. 11 around McMurdo. A full wind barb represents 5 m $s^{-1}$, and the wind speed is shown in shading with the scaling at the bottom. The isolines are sea level pressure with interval of 5 hPa. The McMurdo Station is shown with an asterisk.

observations results in a much improved windstorm intensity forecast at McMurdo.

Of course, one big challenge using the adjoint sensitivity information to improve a specific forecast is that we do not know how much we should change the initial conditions to produce the "right" forecast. Hello et al. (2000) proposed an approach to incorporate sensitive structure in the analyses and proved its efficiency. Combined use of sensitivity information and observations with 3DVAR is a feasible method to improve forecast. Following the approach of Hello et al. (2000), we will also study how quantitatively the modifications of initial conditions can be scaled with the magnitude of sensitivity at each grid point. Using real observations,

such as the global positioning system (GPS) data from the Constellation Observing System for Meteorology, Ionosphere, and Climate, we can perform similar adjoint sensitivity tests and examine their impact.

## 7. Summary and conclusions

With a great effort, WRF tangent linear and adjoint models based on an adiabatic version of WRF model have been developed. TAF greatly reduced the time for the development. The necessary tangent linear and adjoint tests for the developed adiabatic WAMS were passed. The linearity test indicates that the perturbation evolution can be well represented by the WRF tangent linear solutions up to at least 24 h for the 90-km-resolution model.

It is demonstrated that the newly developed adiabatic WAMS can be successfully applied to adjoint sensitivity experiments. In this study, adjoint-based sensitivities have identified the sensitivity regions at 0000 UTC 15 May 2004 in Antarctica in which additional observations, if included in assimilation, may improve the forecast of the windstorm event on 16 May in the McMurdo Station area. Since the magnitudes of partial derivatives of a defined response function with respect to initial conditions directly account for sensitivity, their fields define sensitivity structures, which allow us to investigate spatial patterns of sensitivity variations.

The sensitivity region for the 24-h forecast of the May 2004 McMurdo windstorm lies in the area from the south part of the Trans-Antarctic Mountains to West Antarctica between the Ross Ice Shelf and South Pole. The adjoint sensitivity pattern shows that the analysis underestimates the southerly or southwesterly winds at lower levels on the southern edge of Ross Ice Shelf to West Antarctica. The northeasterly wind at midlevels from the South Pole to Marie Byrd Land should be larger than the analysis. Apart from the wind differences, the pressure low is weaker in the analysis than adjoint sensitivity indicated. The temperature field shows negative sensitivity gradients in the lowest several levels along the international date line between the Ross Ice Shelf and the South Pole, and positive sensitivity at higher levels over the Ross Ice Shelf. On the downward slope of the high land to the Ross Ice Shelf, the temperature in the boundary layer should be reduced while that in the upper levels should be increased, so as to capture the intensity of the windstorm at McMurdo Station. In other words, the atmospheric stratification over the north slope of the Trans-Antarctic Mountain should be more stable than the analysis. Combining the sensitivity analysis of wind and temperature, we conclude that the Froude number should be much larger in the real atmosphere than the analysis.

Numerical experiments with the assimilation of pseudo-observations constructed based on the adjoint gradient information in the sensitivity area indicate that appropriate corrections of the model initial conditions can lead to a significant improvement of the 24-h windstorm prediction at McMurdo. More observations in the sensitivity area are necessary for the weather forecasts in McMurdo and Ross Island. Although pseudo-observations are used, data assimilation experiments indicate that improvement of the forecast from assimilating both wind and temperature observations in the sensitivity area is more beneficial than assimilating only wind or temperature data. The results suggest that a forecast with a specific aspect of interest could resort to the adjoint sensitivity calculation, so as to identify and/or collect more observations in the sensitivity area for analysis of model initial conditions.

We point out that these conclusions are from the adjoint sensitivity point of view. There are other factors that contribute to the failure of the windstorm prediction, such as physics schemes and dealing with terrain in Antarctica in the WRF model. Adjoint sensitivity attributes a specific forecast feature to the model initial conditions. With further improvement of the WRF model, adjoint sensitivity study will identify a more accurate sensitivity pattern and parameters for model initialization in the future.

*Acknowledgments.* We express our sincere appreciation to Bill Skamarock, S. R. Rizvi (NCAR), Thomas Nehrkorn, George Modica (AER), Thomas Kaminski, and Ralf Giering (FastOpt, Germany) for their help during the development of the WRF tangent linear and adjoint models. Discussions with Jordan Powers, Kevin Manning, and Michael Duda (NCAR) were very helpful for this study. We also acknowledge Jordan Powers and Tae-Kwon Wee (NCAR) for their comments and suggestions of our initial manuscript, which greatly improved the presentation of the results. This work is supported by NSF/OPP Grant 0230361.

## REFERENCES

Bromwich, D. H., 1989: Satellite analysis of Antarctic katabatic wind behavior. *Bull. Amer. Meteor. Soc.,* **70,** 738–749.

——, and J. J. Cassano, 2001: Meeting summary: Antarctic weather forecasting workshop. *Bull. Amer. Meteor. Soc.,* **82,** 1409–1413.

——, J. F. Carrasco, and C. R. Stearns, 1992: Satellite observations of Katabatic-wind propagation for great disturbance across the Ross Ice Shelf. *Mon. Wea. Rev.,* **120,** 1940–1949.

——, Y. Du, and T. R. Parish, 1994: Numerical simulation of win-

ter katabatic winds from west Antarctica crossing Siple Coast and the Ross Ice Shelf. *Mon. Wea. Rev.,* **122,** 1417–1435.

Buizza, R., 1994: Sensitivity of optimal unstable structures. *Quart. J. Roy. Meteor. Soc.,* **120,** 429–451.

Burk, S. D., T. Haack, and R. M. Samelson, 1999: Mesoscale simulation of supercritical, subcritical, and transcritical flow along coastal topography. *J. Atmos. Sci.,* **56,** 2780–2795.

Dudhia, J., 1989: Numerical study of convection observed during the winter monsoon experiment using a mesoscale two-dimensional model. *J. Atmos. Sci.,* **46,** 3077–3107.

——, 1993: Nonhydrostatic version of the Penn State–NCAR Mesoscale Model: Validation tests and simulation of an Atlantic cyclone and cold front. *Mon. Wea. Rev.,* **121,** 1493–1513.

Errico, R., 1997: What is an adjoint model? *Bull. Amer. Meteor. Soc.,* **78,** 2577–2591.

——, and T. Vukicevic, 1992: Sensitivity analysis using an adjoint of the PSU–NCAR mesoscale model. *Mon. Wea. Rev.,* **120,** 1644–1660.

Giering, R., and T. Kaminski, 2003: Applying TAF to generate efficient derivative code of Fortran 77-95 programs. *PAMM,* **2** (1), 54–57.

Gilmour, I., L. Smith, and R. Buizza, 2001: On the duration of the linear regime: Is 24 hours a long time in synoptic weather forecasting? *J. Atmos. Sci.,* **58,** 3525–3539.

Grell, G. A., J. Dudhia, and D. R. Stauffer, 1995: A description of the fifth-generation Penn State/NCAR mesoscale model (MM5). NCAR Tech. Note NCAR/TN-398+STR, 122 pp. [Available from UCAR Communications, P. O. Box 3000, Boulder, CO 80307-3000.]

Gustafsson, N., and X.-Y. Huang, 1996: Sensitivity experiments with the spectral HIRLAM and its adjoint. *Tellus,* **48A,** 501–517.

Hello, G., F. Lalaurette, and J.-N. Thépaut, 2000: Combined use of sensitivity information and observations to improve meteorological forecasts: A feasibility study applied to the "Christmas storm" case. *Quart. J. Roy. Meteor. Soc.,* **126,** 621–647.

Hong, S.-Y., Y. Noh, and J. Dudhia, 2006: A new vertical diffusion package with an explicit treatment of entrainment processes. *Mon. Wea. Rev.,* **134,** 2318–2341.

Kleist, D. T., and M. C. Morgan, 2005a: Interpretation of the stucture and evolution of adjoint-derived forecast sensitivity gradients. *Mon. Wea. Rev.,* **133,** 466–484.

——, and ——, 2005b: Application of adjoint-derived forecast sensitivities to the 24–25 January 2000 U. S. East Coast snowstorm. *Mon. Wea. Rev.,* **133,** 3148–3175.

Langland, R. H., R. Gelaro, G. D. Rohaly, and M. A. Shapiro, 1999: Target observations in FASTEX: Adjoint based targeting procedure and data impact experiments in IOP17 and IOP18. *Quart. J. Roy. Meteor. Soc.,* **125,** 3241–3270.

Laprise, R., 1992: The Euler equation of motion with hydrostatic pressure as independent variable. *Mon. Wea. Rev.,* **120,** 197–207.

Li, Z., A. Barcilon, and I. M. Navon, 1999: Study of block onset using sensitivity perturbations in climatological flows. *Mon. Wea. Rev.,* **127,** 879–900.

Mlawer, E. J., S. J. Taubman, P. D. Brown, M. J. Iacono, and S. A. Clough, 1997: Radiative transfer for inhomogeneous atmosphere: RRTM, a validated correlated-k model for the longwave. *J. Geophys. Res.,* **102** (D14), 16 663–16 682.

Navon, I. M., X. Zou, J. Derber, and J. Sela, 1992: Variational data assimilation with an adiabatic version of the NMC spectral model. *Mon. Wea. Rev.,* **120,** 1381–1393.

Parrish, D. F., and J. Derber, 1992: The National Meteorological Center's spectral statistical-interpolation analysis system. *Mon. Wea. Rev.,* **120,** 1747–1763.

Powers, J. G., 2007: Numerical prediction of an Antarctic severe wind event with the Weather Research and Forecasting (WRF) model. *Mon. Wea. Rev.,* **135,** 3134–3157.

——, A. J. Monaghan, C. A. Cayette, D. H. Bromwich, Y.-H. Kuo, and K. W. Manning, 2003: Real-time mesoscale modeling over Antarctica: The Antarctic Mesoscale Prediction System (AMPS). *Bull. Amer. Meteor. Soc.,* **84,** 1533–1546.

Rabier, F., E. Klinker, P. Courtier, and A. Hollingsworth, 1996: Sensitivity of forecast errors to initial conditions. *Quart. J. Roy. Meteor. Soc.,* **122,** 121–150.

Skamarock, W. C., J. B. Klemp, J. Dudhia, D. O. Gill, D. M. Barker, W. Wang, and J. G. Powers, 2005: A description of the advanced research WRF version 2. NCAR Tech. Note NCAR/TN-468+STR, 100 pp. [Available from UCAR Communications, P. O. Box 3000, Boulder, CO 80307-3000.]

Steinhoff, D. F., D. H. Bromwich, M. Lambertson, S. L. Knuth, and M. A. Lazzara, 2008: A dynamical investigation of the May 2004 McMurdo Antarctica severe wind event using AMPS. *Mon. Wea. Rev.,* **136,** 7–26.

Thépaut, J.-N., and P. Courtier, 1991: Four-dimensional data assimilation using the adjoint of a multilevel primitive equation model. *Quart. J. Roy. Meteor. Soc.,* **117,** 1225–1254.

Vukicevic, T., 1991: Nonlinear and linear evolution of initial forecast errors. *Mon. Wea. Rev.,* **119,** 1602–1611.

Xiao, Q., X. Zou, and Y.-H. Kuo, 2000: Incorporating the SSM/I derived precipitable water and rainfall rate into a numerical model: A case study for ERICA IOP-4 cyclone. *Mon. Wea. Rev.,* **128,** 87–108.

——, ——, M. Pondeca, M. A. Shapiro, and C. S. Velden, 2002: Impact of *GMS-5* and *GOES-9* satellite-derived winds on the prediction of a NORPEX extratropical cyclone. *Mon. Wea. Rev.,* **130,** 507–528.

Zou, X., A. Barcilon, I. M. Navon, J. Whittaker, and D. G. Cacuci, 1993: An adjoint sensitivity study of blocking in a two-layer isentropic model. *Mon. Wea. Rev.,* **121,** 2833–2857.

——, F. Vandenberghe, M. Pondeca, and Y.-H. Kuo, 1997: Introduction to adjoint techniques and the MM5 adjoint modeling system. NCAR Tech. Note NCAR/TN-435+STR, 110 pp. [Available from UCAR Communications, P. O. Box 3000, Boulder, CO 80307-3000.]